*CrystEngComm*, 2017,19, 4704-4708 DOI: 10.1039/C7CE01077J

# Molecular recognition and solvatomorphism in a cyclic peptoid: Formation of a stable 1D porous framework.

Eleonora Macedi,[a] Alessandra Meli,[a] Francesco De Riccardis,[a] Patrizia Rossi,[b] Vincent J. Smith,[c] Leonard J. Barbour,[c] Irene Izzo[a,*] and Consiglia Tedesco[a,*]

[a.] *Department of Chemistry and Biology "A. Zambelli", University of Salerno, Via Giovanni Paolo II 132, 84084 Fisciano (SA), Italy.*
[b.] *Department of Industrial Engineering, University of Florence, via S. Marta 3, I-50139 Florence, Italy.*
[c.] *Department of Chemistry and Polymer Science, University of Stellenbosch, Private Bag X1, 7602 Matieland, Stellenbosch, South Africa.*

Electronic Supplementary Information (ESI) available: CCDC 1545931-1545934 contain the supplementary crystallographic data for this paper.

**Molecular recognition and the hydrophobic effect explain the solvatomorphic behavior of a hexameric α-cyclic peptoid. Either a pure non-porous crystal form or a stable one-dimensional porous framework is obtained by appropriate choice of crystallization solvents.**

The study of molecular aggregation in solution to form crystalline solids represents the focus of interdisciplinary research efforts.[1,2] An understanding of the supramolecular aspects in the nucleation step is crucial to control the overall outcome of the crystallization process. A holistic approach takes into account both the structural diversity and the possible interaction patterns of the involved species to exploit the chemistry of nucleation.[3] In particular, a recent total scattering study demonstrated that solvent molecules restructure around the forming nanoparticles depending on the nature of the counterparts.[4] Thus, the solvent plays a key role in determining the resulting crystal form.[5] Conformational flexibility adds further complexity to the crystallization process, giving rise to conformational polymorphs that differ not only in the packing mode, but also in the molecular conformation.[6]

In our ongoing studies on cyclic peptoids[7-10] we have investigated the role of the crystallization solvent in the solid state assembly of the cyclic hexamer cyclo-(Nme-Npa$_2$)$_2$ (compound **1** in Scheme 1, Nme = N-(methoxyethyl)glycine, Npa = N-(propargyl)glycine) and reported its peculiar solid state dynamics.[11] Compound **1** crystallizes from acetonitrile as form **1A** and undergoes a reversible single-crystal-to-single-crystal transformation upon release of guest molecules with a drastic conformational change to give the desolvated crystal form **1B**.[11] In form **1A** methoxyethyl and propargyl side chains extend vertically with respect to the macrocycle plane, inducing the columnar arrangement of the peptoid macrocycles. Upon acetonitrile removal two vertical propargyl side chains tilt by 113° and form an unprecedented CH-pi zipper that links together the peptoid columns in the desolvated crystal form **1B**. Thereafter, upon exposure to acetonitrile molecules the CH-pi zipper opens up and transforms back to the solvated form **1A**.[11] Subsequent to these intriguing results, we report herein a polymorph screening of compound **1** with a view to understanding the role of the crystallization solvent in the solid state assembly (Scheme 1). In particular, we obtained and characterized two new crystal forms of **1,** namely **1C** and **1D**. We were also able to derive two other crystal forms **1E** and **1F** from **1D**, with the latter **1F** being a stable empty porous form.

**1C** and **1D** were crystallized by slow evaporation from acetonitrile/water and acetonitrile/methanol solutions, respectively (Scheme 1, see ESI for further details).

Single crystal X-ray diffraction‡ (see also Fig. S1-S3 and Table S1, ESI) showed that **1C** crystallizes as a pure form, while **1D** is a methanol solvate. In both crystal forms the macrocycle possesses a crystallographic inversion centre and exhibits a distorted *cctcct* peptoid backbone conformation (where *c* denotes *cis*, and *t trans*).[12]

Nevertheless the macrocycle conformation in **1C** and **1D** is remarkably different: in **1C** two propargyl residues feature a *trans* conformation while in **1D** the methoxyethyl residues correspond to the *trans* residues, as observed in crystal forms **1A** and **1B** (Fig. 1 and Fig. S4-S6, ESI).[11]

Gas phase energy optimization[13] indicates that the novel molecular conformation observed in crystal form **1C** is less stable by 30 kJ/mol with respect to that of **1D** (see ESI for details).

Hirshfeld surface analysis[14] and lattice energy calculations using the PIXEL method[15] allowed us to quantitatively assess the main assembly motifs in the two crystal forms (Fig. 1 and Fig. S7-S9 and Tables S2-S3 ESI).

In **1C** a layered arrangement in the plane *ab* is provided by backbone-to-side chains CO···H$_2$C interactions involving the *cis* carbonyl groups and both propargyl residues (Fig. 1C, S7c, S8 and motifs I and II in Table S2, ESI). In **1D** a columnar arrangement along the shortest axis is provided by backbone-to-side chain CO···HC≡C interactions involving the *trans* carbonyl groups and the vertical *cis* propargyl side chains (Fig. 1D, S7d, S9 and motif I in Table S3, ESI). Vertical propargyl side chains act as pillars and extend vertically with respect to the macrocycle plane interacting with the backbone atoms of the macrocycles below and above, as previously observed.[8-9,10a,11]

In **1C** layers are interconnected along the *c* axis by backbone-to-side chain interactions by means of C=O···H-C≡C and pi-pi interactions involving the *cis* propargyl side chains (Fig. S8 and motifs III and IV in Table S2). In **1D** intercolumnar interactions are provided by backbone-to-side chain C=O···H-C≡C

interactions and involve the horizontal propargyl side chains (Fig. S9 and motif II in Table S3, ESI).

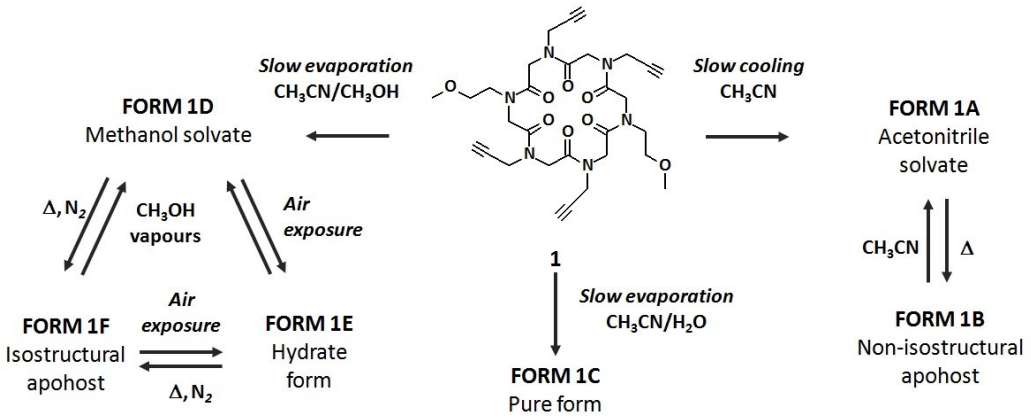


**Scheme 1.** Crystal forms of cyclo-(Nme-Npa$_2$)$_2$ **1**, Nme = N-(methoxyethyl)glycine, Npa = N-(propargyl)glycine.

Thus, we obtained two different molecular conformations in crystal forms **1C** and **1D** by changing the molecular environment during the crystallization process. In particular, adding water to the crystallization solvent triggers a new conformation induced by a hydrophobic effect. In **1C** the more hydrophilic methoxyethyl side chains are oriented horizontally with respect to the macrocycle plane and are more exposed with respect to **1D**, where the methoxyethyl side chains are vertical and eventually embedded in the cyclopeptoid columns (Fig. 1 and S7c-d, ESI). Moreover, the layered assembly in **1C** allows to maximize the interactions among the hydrophobic propargyl side chains.

Adding methanol to the acetonitrile solution does not have the same conformational effect observed in **1C**; indeed the molecular conformation is the same obtained in **1A** using only acetonitrile as the crystallization solvent.[16] Methanol molecules in form **1D** occupy cavities between the columns (with a volume of 84.4 Å$^3$ per unit cell,[17] Fig. 2 and 3b) and are hydrogen bonded to the *cis* carbonyl oxygen atoms O2 (CO···HO 1.79 Å, CO···HO 173.4°). The carbonyl oxygen atoms O2 act as H-bond binding sites (Fig. S7d ESI). Indeed, acetonitrile molecules in form **1A** occupy channels (with a volume of 196.2 Å$^3$, Fig. 2 and 3a) and bind to the *cis* carbonyl oxygen atoms O3 (CO···HC 2.65 Å, CO···HO 157.1°, Fig. S7a ESI). Notably, the assembly of columns in **1D** and **1A** is different, as intercolumnar interactions in **1D** and **1A** are mediated by the guest molecules, which are attached to different sides of the columns (Fig. 2). In **1D** the columns pack in an approximate hexagonal arrangement and in **1A** the columns shifted by one half along the shortest cell axis.

Thermal analyses were carried out for both crystal forms. In the case of **1C**, DSC shows that the sample is stable up to 190 °C, and decomposes thereafter (Fig. S10, ESI).

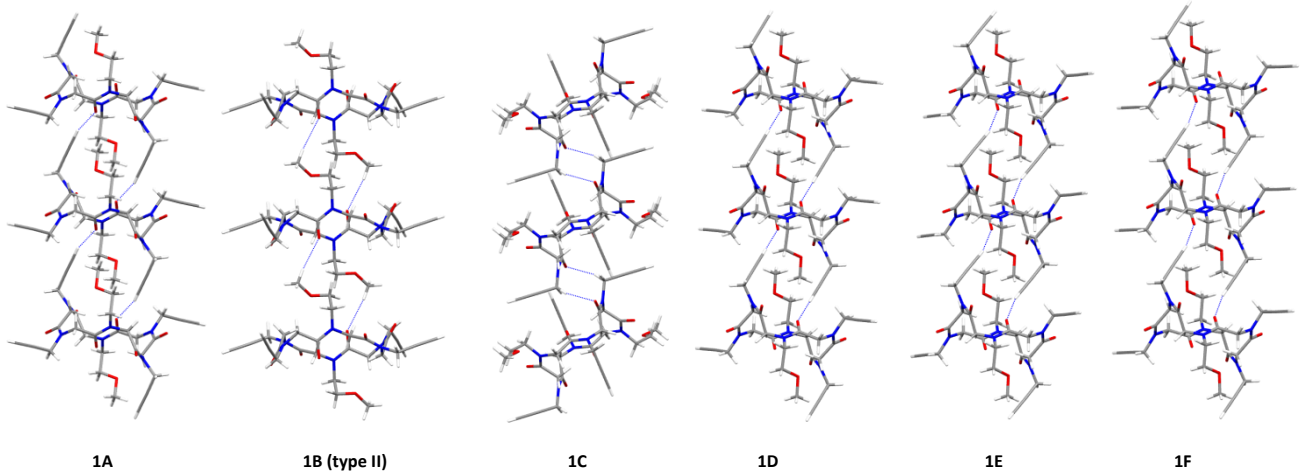


**Fig. 1** Arrangement of cyclopeptoid molecules along the shortest crystallographic axis in crystal forms **1A**, **1B** type **II** molecules, **1C**, **1D**, **1E** and **1F**. C=O···H-C hydrogen bonds are depicted as dotted lines. Atom types: C grey, N blue, O red, H white.

For **1D**, DSC and TGA reveal that desolvation occurs in one step over a wide temperature range from 30 °C to 90 °C (Fig. S11 and S12, ESI). DSC also shows two closely occurring endothermic and exothermic events, starting at 184 °C and 215 °C, respectively. Finally, decomposition occurs at T > 230 °C (Fig. S11, ESI).

The observed percentage weight loss of 8.2% from TGA corresponds to 1.7 molecules of methanol per cyclopeptoid molecule, which is in agreement with the value determined from single crystal X-ray structure analysis.‡

It is noteworthy that a single crystal of form **1D,** exposed to air at room temperature for 30 minutes, is able to exchange the methanol molecules with water molecules (as shown by single crystal X-ray diffraction), resulting in the crystal form **1E**. Crystal form **1E** is isostructural with **1D**‡ (Fig. 2). The cyclopeptoid molecules in the two crystal forms overlap with a rmsd value of 0.1904 Å. Water molecules in form **1E** occupy the cavities (with a volume of 11.9 Å$^3$, Fig. 3c) between the columns and are hydrogen bonded to the *cis* carbonyl oxygen atoms O2 (CO···HO distance 1.92 Å, CO···HO angle 166.7°). The carbonyl oxygen atoms O2 again act as H-bond binding sites (Fig. S7e, ESI).

To test the crystal stability in the absence of guest molecules, an *in situ* variable temperature single crystal X-ray diffraction experiment was performed (see ESI for details). A fresh crystal of **1D** was flash cooled in liquid nitrogen and analyzed at 100 K to confirm the presence of methanol molecules, it was then heated using a hot air blower and measured at 323 K, 368 K, 393 K and cooled back to 100 K. The structure determinations revealed that methanol molecules left the crystal at 323 K to give rise to the isostructural apohost **1F**.

Importantly, the columnar architecture remains intact and voids form (with a volume of 14.6 Å$^3$, Fig. 3d), showing the robustness of the framework upon solvent removal. Form **1F** remains stable in a nitrogen atmosphere from 100 K to 393 K.

When exposed to environmental humidity the apohost **1F** gives form **1E,** meaning that the cavities are accessible to incoming and outgoing guest molecules.

Form **1F** shows a lower packing coefficient (0.706) than the solvated crystal forms **1D** (0.766), **1E** (0.758) and **1A** (0.769). In **1C** the packing coefficient is 0.724, indicating that host-guest interactions in **1D** and **1E** favor a more efficient packing arrangement.

We also verified the reversibility of the exchange process between water and methanol molecules by an *in situ* single crystal XRD experiment, exposing a crystal of **1E** to methanol vapours in a capillary (see ESI). Structural analysis confirmed the transformation to form **1D**. Notably the cavities contract considerably when they are occupied by water molecules (11.9 Å$^3$) instead of methanol molecules (84.4 Å$^3$). However, the volume of the cavities (14.6 Å$^3$) in the empty form **1F** does not change significantly with respect to the hydrate form **1E**.

In conclusion, the conformational flexibility of compound **1** is crucial to the observed solvatomorphism. The crystallization solvents are able to favour one conformation over the other, leading either to a one-dimensional columnar (**1A** and **1D**) or a two-dimensional layered assembly of cyclopeptoid molecules (**1C**). Once the columns are formed, they may assemble in different ways and the interaction with the guest molecules such as acetonitrile or methanol drives the final assembly in the solid state, leading to a different sorption behavior.

Indeed, compound **1** exhibits two different possible guest release and uptake mechanisms according to the exhibited crystal form:

- in **1A**, the host framework releases the guest molecules, yielding the non-isostructural apohost **1B**, which in turn adsorbs the incoming guest and transforms back to **1A**.[11]
- in **1D** and **1E**, the host framework releases the guest molecules to give a zeolite-like isostructural apohost **1F**, with stable cavities open to incoming and outgoing guest molecules.

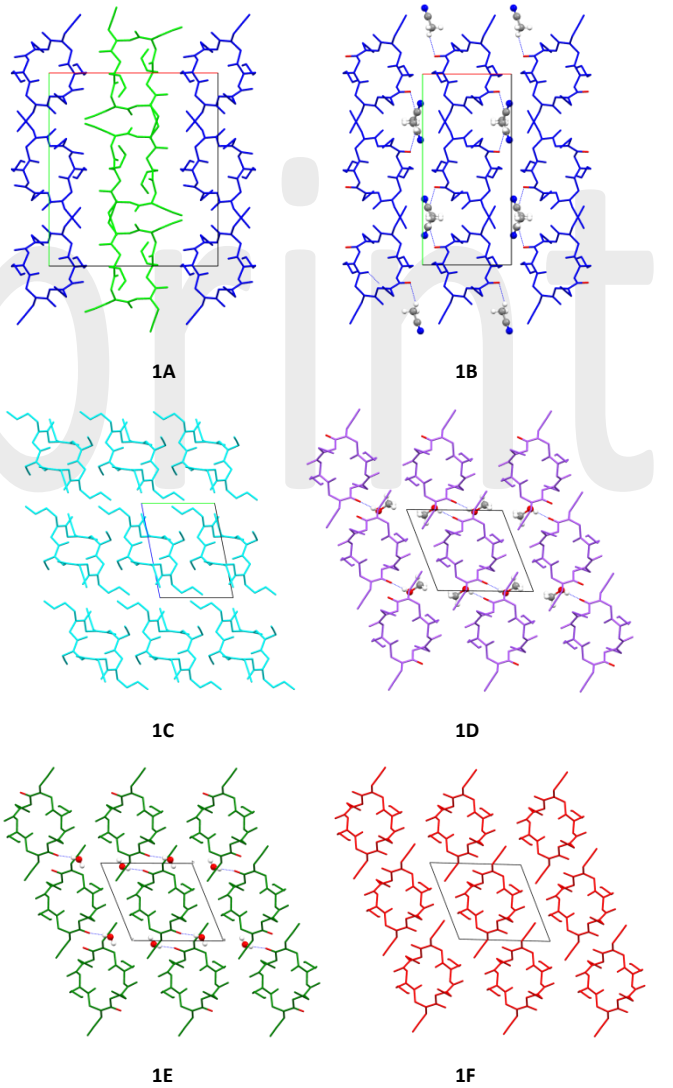


**Fig. 2** Crystal packing of crystal forms **1A**, **1B** (type **I** molecules in blue; type **II** molecules in green), **1C**, **1D**, **1E** and **1F** as viewed along the shortest crystallographic axis. Host binding sites are highlighted in red. guest molecules are depicted as ball and stick. Hydrogen atoms are visualized only for guest molecules.

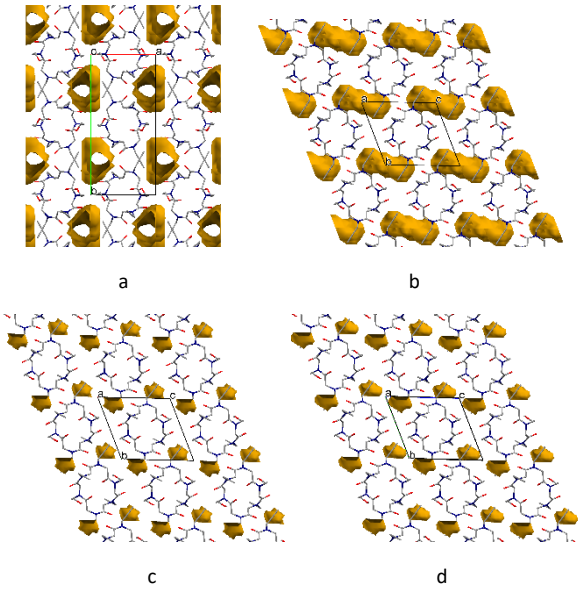


**Fig. 3** Contact surfaces (yellow) in the crystal structures of **1** (probe radius: 1.2 Å). a) Form **1A**: channels (V = 196.2 Å$^3$ per unit cell) parallel to the *c* axis; b) form **1D**: cavities (V = 84.4 Å$^3$) stacked along the *c* axis; c) form **1E**: cavities (V = 11.9 Å$^3$) stacked along the *c* axis; d) form **1F**: cavities stacked along the *c* axis (V = 14.6 Å$^3$).

Finally, compound **1** represents a paradigmatic example of how conformational changes are induced by the external environment, leading to different aggregation modes with divergent properties, paving the way to the understanding of a similar behavior in more complex systems as polypeptides.

The research leading to these results has received funding from the University of Salerno (FARB) and the People Programme (Marie Curie Actions) of the European Union's Seventh Framework Programme FP7/2007-2013/ under REA grant agreement n°PIRSES-GA-2012-319011. COST Action CM1402 Crystallize is acknowledged. We are grateful to Prof. R. Zanasi (Univ. of Salerno) for valuable discussions and to Centro di Cristallografia Strutturale (Univ. of Florence) for access to X-ray facilities.

## Notes and references

‡ Crystal data for **1C**. *T*= 296 K, formula: $C_{30}H_{38}N_6O_8$, FW= 610.66, triclinic, space group $P\bar{1}$, *Z*= 1, *a*= 8.814(3) Å, *b*= 9.0944(18) Å, *c*= 10.982(4) Å, $\alpha$= 78.86(2)°, $\beta$= 87.55(3)°, $\gamma$= 66.35(2)°, *V*= 790.6(4) Å$^3$, $D_x$= 1.283 g cm$^{-3}$, $\mu_{calc}$= 0.094 mm$^{-1}$, $F_{000}$= 324.0, $R(I > 2\sigma_I)$= 0.0762(1454), $_wR_2$= 0.2567(3541), N. of param.= 200, GooF= 0.986, $\rho_{min}$, $\rho_{max}$= -0.22, 0.33 eÅ$^{-3}$.
Crystal data for **1D**. *T*= 100 K, formula: $C_{30}H_{38}N_6O_8{\cdot}1.76\ CH_3OH$, FW= 667.06, triclinic, space group $P\bar{1}$, Z= 1, *a* = 8.5007(14) Å, *b*= 10.3965(11) Å, *c*= 10.9102(17) Å, $\alpha$= 67.863(11)°, $\beta$= 84.552(15)°, $\gamma$= 71.048(13)°, *V*= 844.3(2) Å$^3$, $D_x$ = 1.312 g cm$^{-3}$, $\mu_{calc}$= 0.098 mm$^{-1}$, $F_{000}$= 356.0, $R(I > 2\sigma_I)$= 0.0713(2056), $_wR_2$= 0.2158(3799), N. of param.= 221, GooF= 0.966, $\rho_{min}$, $\rho_{max}$= -0.31, 0.37 eÅ$^{-3}$.
Crystal data for **1E**. *T*= 100 K, formula: $C_{30}H_{38}N_6O_8{\cdot}H_2O$, FW= 628.68, triclinic, space group $P\bar{1}$, *Z*= 1, *a*= 8.5852(15) Å, *b*= 10.4929(17) Å, *c*= 10.556(2) Å, α= 68.110(9)°, $\beta$= 86.318(10)°, $\gamma$= 67.035(9)°, *V*= 808.8(3) Å$^3$, $D_x$= 1.291 g cm$^{-3}$, $\mu_{calc}$= 0.096 mm$^{-1}$, $F_{000}$= 334.0, R($I > 2\sigma_I$)= 0.0601(1780), $_wR_2$= 0.1806(3241), N. of param.= 214, GooF= 0.953, $\rho_{min}$, $\rho_{max}$= -0.31, 0.27 eÅ$^{-3}$.
Crystal data for **1F**. *T*= 100 K, formula: $C_{30}H_{38}N_6O_8$, FW= 610.66, triclinic, space group $P\bar{1}$, Z = 1, *a*= 8.5875(8) Å, *b*= 10.3508(8) Å, *c*= 10.6762(8) Å, α= 67.884(7)°, $\beta$= 86.630(7)°, γ= 68.351(8)°, *V*= 813.60(13) Å$^3$, $D_x$= 1.246 g cm$^{-3}$, $\mu_{calc}$= 0.092 mm$^{-1}$, $F_{000}$= 324.0, $R(I > 2\sigma_I)$= 0.0492(2051), $_wR_2$= 0.1099(3081), N. of param.= 199, GooF= 1.020, $\rho_{min}$, $\rho_{max}$= -0.21, 0.23 eÅ$^{-3}$.

1 A. Gavezzotti, *Molecular aggregation, structure analysis and molecular simulation of crystals and liquids*, Oxford University Press, Oxford, 2nd ed., 2007.
2 J. W. Mullin, *Crystallization,* Butterworth-Heinemann, Oxford, 4th ed., 2001.
3 E. D. Bøjesen and B. B. Iversen, *CrystEngComm*, 2016, **18**, 8332–8353.
4 M. Zobel, R. B. Neder and S. A. J. Kimber, *Science*, 2015, **347**, 292–294.
5 L. R. Nassimbeni, *Acc. Chem. Res.*, 2003, **36**, 631–637.
6 A. J. Cruz-Cabeza and J. Bernstein, *Chem. Rev.*, 2014, **114**, 2170−2191.
7 For recent reviews on peptoids see: (a) N. Gangloff, J. Ulbricht, T. Lorson, H. Schlaad and R. Luxenhofer, *Chem. Rev.*, 2016, **116**, 1753−1802; (b) J. Sun and R. N. Zuckermann, *ACS Nano*, 2013, **7**, 4715–4732; (c) I. Izzo, C. De Cola and F. De Riccardis, *Heterocycles*, 2011, **82**, 981–1006; (d) A. S. Culf, R. J. Ouellette, *Molecules*, 2010, **15**, 5282–5335.
8 C. Tedesco, L. Erra, I. Izzo and F. De Riccardis, *CrystEngComm*, 2014, **16**, 3667–3687.
9 C. Tedesco, A. Meli, E. Macedi, V. Iuliano, A. G. Ricciardulli, F. De Riccardis, G. Vaughan, V. J. Smith, L. J. Barbour and I. Izzo, *CrystEngComm*, 2016, **18**, 8838–8848.
10 (a) C. Tedesco, E. Macedi, A. Meli, G. Pierri, G. Della Sala, C. Drathen, A. N. Fitch, G. B. M. Vaughan, I. Izzo and F. De Riccardis, *Acta Cryst.* B 2017, **73**, 399−412; (b) R. Schettini, F. De Riccardis, G. Della Sala and I. Izzo, *J. Org. Chem.*, 2016, **81**, 2494–2505; (c) C. De Cola, G. Fiorillo, A. Meli, S. Aime, E. Gianolio, I. Izzo and F. De Riccardis *Org. Biomol Chem.* 2014, **21**, 424–431; (d) I. Izzo, G. Ianniello, C. De Cola, B. Nardone, L. Erra, G. Vaughan, C. Tedesco and F. De Riccardis, *Org. Lett.*, 2013, **15**, 598–601; (e) N. Maulucci, I. Izzo, G. Bifulco, A. Aliberti, C. De Cola, D. Comegna, C. Gaeta, A. Napolitano, C. Pizza, C. Tedesco, D. Flot and F. De Riccardis, *Chem. Commun*., 2008, 3927–3929.
11 A. Meli, E. Macedi, F. De Riccardis, V. J. Smith, L. J. Barbour, I. Izzo and C. Tedesco, *Angew. Chem., Int. Ed.*, 2016, **55**, 4679–4682.
12 Peptoid backbones of **1C** and **1D** overlap within a rmsd value of 0.062 Å (Fig. S4, ESI). In both cases, the macrocycle has an approximately rectangular shape (Fig. S5, ESI). The backbone conformation could mimic a $\beta$-turn structure as reported by (a) B. Yoo, S. B. Y. Shin, M. L. Huang and K. Kirshenbaum, *Chem. Eur. J.*, 2010, **16**, 5528–5537; (b) S. B. Y. Shin, B. Yoo, L. J. Todaro and K. Kirshenbaum, *J. Am. Chem. Soc.*, 2007, **129**, 3218–3225.
13 M. J. Frisch *et al.,* Gaussian 09, revision A.1; Gaussian, Inc.; Wallingford, CT, 2009.
14 (a) M. A. Spackman and D. Jayatilaka, *CrystEngComm*, 2009, **11**, 19–32; (b) J. J. McKinnon, M. A. Spackman and A. S. Mitchell, *Acta Crystallogr., Sect. B: Struct. Sci*., 2004, **60**, 627–668; (c) M. A. Spackman and J. J. McKinnon, *CrystEngComm*, 2002**, 4**, 378–392.
15 A. Gavezzotti, *New J. Chem.*, 2011, **35**, 1360–1368; (b) A. Gavezzotti, *J. Phys. Chem. B*, 2003, **107**, 2344–2353; (c) A. Gavezzotti, *J. Phys. Chem. B*, 2002, **106**, 4145–4154.
16 The cyclopeptoid molecules in **1A** and **1D** overlap within a rmsd of 0.331 Å.
17 C. F. Macrae, I. J. Bruno, J. A. Chisholm, P. R. Edgington, P. McCabe, E. Pidcock, L. Rodriguez-Monge, R. Taylor, J. van de Streek and P. A. Wood, *J. Appl. Crystallogr*., 2008, **41**, 466–470.